J. Am. Chem. Soc. **2001,** *123,* 4749−4754

Supramolecular Origins of Product Selectivity for Methanol-to-Olefin Catalysis on HSAPO-34

Weiguo Song, Hui Fu, and James F. Haw*

Contribution from the Loker Hydrocarbon Research Institute and Department of Chemistry, University of Southern California, University Park, Los Angeles, California 90089-1661

Received November 29, 2000

Abstract: Ethylene selectivity in methanol-to-olefin (MTO) catalysis is related to the number of methyl groups on benzene rings trapped in the nanocages of the preferred catalyst HSAPO-34. By correlating the time evolutions of the catalysts' ^{13}C NMR spectra and the volatile product distribution following abrupt cessation of methanol flow, we discovered that (in the absence of other adsorbates) propene is favored by methylbenzenes with four to six methyl groups but ethylene is predominant from those with two or three methyl groups. We substantially increased ethylene selectivity by operating at lower methanol partial pressures or higher temperatures, either of which reduces the steady-state average methyl substitution. As a step toward a kinetic analysis of the MTO reaction on HSAPO-34, we treated each nanocage with a methylbenzene molecule as a supramolecule capable of unimolecular dissociation into ethylene or propene and a less highly substituted methylbenzene. Addition of a water molecule to a nanocage containing a methylbenzene produces a distinct supramolecule with unique properties. Indeed, co-feeding water with methanol significantly increased the average number of methyl groups per ring at steady state relative to identical conditions without additional water, and also increased ethylene selectivity, apparently through transition state shape selectivity.

Introduction

Control of selectivity is a central problem in catalysis, and this is particularly challenging with the microporous solid acid catalysts[1−3] used in most industrial catalytic processes. We recently demonstrated that for some reactions on solid acids, the active site is a hybrid of inorganic and cyclic organic components.[4,5] The latter function as scaffolds for bond making and breaking steps that would otherwise be energetically unfavorable. In the case of methanol-to-olefin (MTO) conversion[6] on the preferred catalyst HSAPO-34 (a silico-aluminophosphate of CHA topology),[7] the organic components are methylbenzenes[8] that self-assemble in the nanometer-size cages during a kinetic induction period, where they must remain until burned out, as even benzene is too large to pass through the 0.38 nm windows connecting adjacent cages. An outstanding problem in MTO catalysis is improving ethylene selectivity at the expense of propene to better match the demand for the corresponding polyolefins.

Here we show that ethylene selectivity is governed by the number of methyl substituents on the aromatic rings, and the presence or absence of other molecules in the nanocages. At higher methanol space velocities (partial pressures), the average number of methyl groups per ring reaches a steady-state value of greater than 5 at 400 °C, and the ethylene selectivity is only ca. 25%. At far lower space velocities, the average number of methyl groups per ring reaches a steady-state value below 2, and the catalyst then yields over 60% ethylene. Similarly, the average number of methyl groups per ring reaches lower steady-state values at higher temperatures, and this contributes to higher ethylene selectivities.

As a step toward a kinetic analysis of MTO chemistry in HSAPO-34, we treat each nanocage containing a methylbenzene as an independent supramolecule capable of unimolecular decomposition to either ethylene, $\{n\} \rightarrow \{n-2, \mathrm{e}\}$, or propene, $\{n\} \rightarrow \{n-3, \mathrm{p}\}$, where n implies a methylbenzene molecule with n methyl groups, and $\{\ \}$ designates the nanocage and its associated Brønsted acid site. We performed a series of experiments where we allowed a working catalyst to reach steady state during continuous introduction of methanol before abruptly cutting off reagent introduction. We then followed the time evolutions of the rates of product formation and the average number of methyl groups on benzenes trapped in the catalyst's nanocages. The correlation of these observables permitted us to compare the relative magnitudes of some of the unimolecular rate constants for the reactions for supramolecules composed of cages containing a methylbenzene molecule, but no other adsorbate. A rate equation is derived to account for the time evolution of the average number of methyl groups per benzene ring in such experiments.

Coadsorption of a water molecule into a nanocage with a methylbenzene produces unique supramolecules, $\{n, \mathrm{H_2O}\}$, and we find that rate constants for their decomposition to olefinic

---

[1] VanSanten, R. A.; Kramer, G. J. *Chem. Rev.* **1995**, *95*, 637−660.

[2] Corma, A. *Chem. Rev.* **1995**, *95*, 559−614.

[3] Corma, A. *Chem. Rev.* **1997**, *97*, 2373−2419.

[4] Haw, J. F.; Nicholas, J. B.; Song, W.; Deng, F.; Wang, Z.; Heneghan, C. S. *J. Am. Chem. Soc.* **2000**, *122*, 4763−4775.

[5] Song, W.; Haw, J. F.; Nicholas, J. B.; Heneghan, K. *J. Am. Chem. Soc.* **2000**, *122*, 10726−10727.

[6] Stöcker, M. *Microporous Mesoporous Mater.* **1999**, *29*, 3−48.

[7] Wilson, S.; Barger, P *Microporous Mesoporous Mater.* **1999**, *29*, 117−126.

[8] Toluene has also been implicated as a "cocatalyst" for methanol conversion on aluminosilicate zeolites: (a) Mole, T.; Whiteside, J. A.; Seddon, D. *J. Catal.* **1983**, *82*, 261−266. (b) Mole, T.; Bett, G.; Seddon, D. *J. Catal.* **1983**, *84*, 435−445. Other workers have proposed a phenomenological carbon-pool mechanism for MTO chemistry on HSAPO-34 without explicitly identifying the organic species responsible for the catalytic effect: (c) Dahl, I. M.; Kolboe, S. *J. Catal.* **1996**, *161*, 304−309. (d) Dahl, I. M.; Kolboe, S. *J. Catal.* **1994**, *149*, 458−464.

10.1021/ja0041167 CCC: $20.00

products, for example, $\{n, H_2O\} \rightarrow \{n-2, H_2O, e\}$ are slower than in the absence of water, leading to higher steady-state averages for the number of methyl groups per benzene rings. Furthermore, the presence of water in the nanocage significantly increases ethylene selectivity at the expense of propene, and we attribute this to enhanced transition state shape selectivity.

Experimental Section

Materials and Reagents. HSAPO-34 was prepared according to a patent procedure.[9] XRD showed a pure crystalline phase with the CHA structure. The product was calcined at 873 K for 10 h to remove the template agent and pressed into 10−20 mesh pellets. The Brønsted site concentration was determined to be 1.1 mmol/g. Methanol-^{13}C was obtained from Isotech, Inc. In general, we used methanol-^{13}C for experiments in which an NMR measurement was to be made (with or without GC) and natural abundance methanol if GC was to be the only analytical method.

Catalysis. Experiments were performed by using the pulse quench reactor described elsewhere[10] with the exception that methanol was delivered by a motor-driven syringe pump (Harvard Apparatus model PHD 2000). For each experiment a bed consisting of 0.3 g of catalyst was activated at 673 K in the reactor under 200 sccm He flow for 2 h immediately prior to use. This carrier gas feed rate was also used during methanol introduction in all experiments. For NMR sample preparation, methanol flow was abruptly ceased a predetermined time (usually 0 to 60 min) prior to quench. Previous studies have shown that the temperature of the catalyst pellets decreases 150 K in the first 170 ms of a quench. After quenching each reacted catalyst sample, the reactor was sealed off and transferred into a glovebox filled with nitrogen. The catalyst pellets were ground and transferred to a 7.5-mm MAS rotor that was sealed with a Kel-F end-cap.

Gas Chromatography. A Hewlett-Packard Model 6890 gas chromatograph with flame-ionization detector was used to analyze gases sampled from the reactor product streams with a Valco valve. The column was 150 m dh150 (Supelco) operated isothermally at 323 K to permit sampling of the gas stream more frequently than the total analysis time for any given sample.

NMR Spectroscopy. ^{13}C solid-state NMR experiments were performed with magic angle spinning (MAS) on a modified Chemagnetics CMX-300 MHz spectrometer operating at 75.4 MHz for ^{13}C. Hexamethylbenzene (17.4 ppm) was used as an external chemical shift standard, and all ^{13}C chemical shifts are reported relative to TMS. Chemagnetics-style pencil probes spun 7.5 mm zirconia rotors at typically 6.5 kHz with active spin speed control (±3 Hz).

Typical ^{13}C experiments included the following: cross polarization (CP, contact time = 2 ms, pulse delay = 1 s, 2000 transients); cross polarization with interrupted decoupling (contact time = 2 ms, pulse delay = 1 s, 2000 transients, dipolar dephasing time of 50 μs); and single pulse excitation with proton decoupling (Bloch decay, pulse delay = 10 s, 400 transients). CP and Bloch decay spectra gave very similar values for the average number of methyl groups per aromatic ring. Similar to other NMR work on chemically dilute carbonaceous materials, the CP spectra here were generally "cleaner" than the Bloch decay spectra. All spectra reported here were measured with CP, but the average methyl group numbers reported were determined from the Bloch decay spectra since these are more commonly regarded as quantitative. Our conclusions would not change if we reported integrations from the CP spectra.

Results

Decomposition of Methylbenzenes Following Methanol Cutoff. We carried out a series of experiments in which we first flowed 0.1 mL of methanol or methanol-^{13}C onto a 300 mg bed of pelletized HSAPO-34 at 400 °C at a weight hourly space velocity (WHSV) of 8 h^{-1} (for a 300 mg catalyst bed this corresponds to 50 μL/min) before abruptly terminating methanol flow and waiting a variable time before quenching the catalyst temperature to ambient. Figure 1 reports solid-state ^{13}C MAS NMR spectra of catalysts prepared with delays from 0 to 60 min. These spectra show an aromatic carbon signal between 129 and 134 ppm, and a methyl group resonance at 20 ppm that drops with increasing delay between methanol cutoff and thermal quench. A small, sharp resonance at 25 ppm is due to isobutane, which like the methylbenzenes, is too large to exit the nanocages.

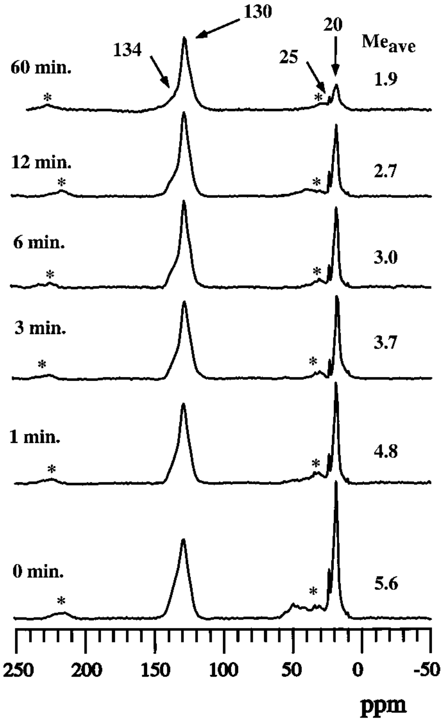

Figure 1. ^{13}C CP/MAS NMR spectra (75 MHz) showing the loss of methyl groups as a function of time from methylbenzenes trapped in the HSAPO-34 nanocages at 400 °C. For each case, a fresh catalyst bed was used to convert 0.1 mL of methanol-^{13}C at a WHSV of 8 h^{-1}, and then methanol flow was abruptly cut off. The catalyst bed was maintained at temperature with He flow (200 sccm) for the time indicated, and then the reactor temperature was rapidly quenched to ambient. Entire catalyst beds were loaded into MAS rotors to avoid sampling errors, and cross polarization spectra were measured at room temperature. The average numbers of methyl groups per ring, Me$_{ave}$, were calculated from Bloch decay spectra very similar to the cross polarization spectra shown.

The ^{13}C NMR spectra permit direct measurement of the average number of methyl groups per benzene ring in the catalyst, Me$_{ave}$.

$$\mathrm{Me}_{ave} = [\text{methyls}]/[\text{rings}] = \sum_{n=0}^{6} n f_n \qquad (1)$$

f_n denotes the fractions of rings with n methyl groups. As shown in Figure 1, Me$_{ave}$ decreased from a nearly full complement of 5.6 immediately after methanol cutoff to 1.9 (e.g., xylenes on average) after 60 min. The last methyl group could be removed only with great difficulty. At 450 °C, Me$_{ave}$ was 1.1 after 60 min and 0.2 after 14 h.

Figure 2 reports gas chromatographic analyses of samples taken from the product streams immediately prior to thermal

---

[9] Lok, B. M.; Messina, C. A.; Patton, R. L.; Gajek, R. T.; Cannan, T. R.; Flanigen, E. M. U.S. Patent 4,440,871, 1984.

[10] (a) Haw, J. F.; Goguen, P. W.; Xu, T.; Skloss, T. W.; Song, W.; Wang, Z. *Angew. Chem.* **1998**, *37*, 948−949. (b) Goguen, P. W.; Xu, T.; Barich, D. H.; Skloss, T. W.; Song, W.; Wang, Z.; Nicholas, J. B.; Haw, J. F. *J. Am. Chem. Soc.* **1998**, *120*, 2651−2652. (c) Xu, T.; Barich, D. H.; Goguen, P. W.; Song, W.; Wang, Z.; Nicholas, J. B.; Haw, J. F. *J. Am. Chem. Soc.* **1998**, *120*, 4025−4026.

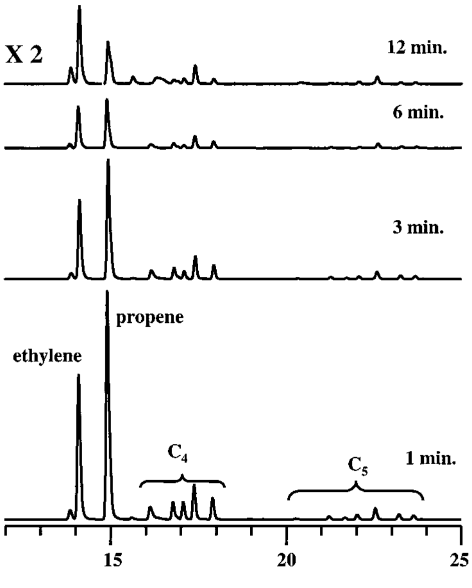

Figure 2. Gas chromatography (flame-ionization detection) analyses of the volatile products captured immediately prior to thermal quench from the experiments used to prepare some of the samples for Figure 1. Note the significant increase in ethylene selectivity at longer times.

quench for several of the experiments used to prepare the samples for Figure 1. One minute after methanol cutoff, the catalyst was still producing olefinic products with an ethylene selectivity only slightly higher than that immediately prior to cutoff; in particular, one notes a much higher selectivity for propene than for ethylene. As the catalyst continued to age at 400 °C with He flow but no further addition of methanol, the total rate of olefin production necessarily fell, but the ethylene selectivity increased dramatically, surpassing that of propene between 6 and 12 min after cutoff. We measured the rates of formation of ethylene, propene, and a representative C_4 product from a single experiment in which we made a number of gas chromatographic injections as a function of time, and these data are plotted in Figure 3a; ethylene dominated after 8 min. C_4 products may form in part from secondary reactions and are hereafter neglected. Figure 3b compares the ethylene and propene selectivities, computed from Figure 3a, as a function of the time evolution of the average number of methyl groups per ring: a mapping made possible by a smooth fit of the data in Figure 1. The relationship between molecular structure and selectivity is clear, a changeover in selectivity to ethylene occurred when the number of methyl groups per ring decreased to 2.8, and further decreases in propene selectivity accompanied further decreases in methyl substitution.

Effects of Space Velocity or Temperature. We explored rational means of limiting the average number of methyl groups per ring to see if these conditions did indeed increase ethylene selectivity. Figure 4 reports ^{13}C NMR spectra that demonstrate that as the methanol space velocity (and hence partial pressure) was reduced at 400 °C, the benzene rings reached steady state with fewer methyl groups per ring. The figure shows that as the space velocity was decreased (at 400 °C) from 8 h^{-1} to 0.0008 h^{-1}, Me$_{ave}$ decreased progressively from 5.6 to 1.2.

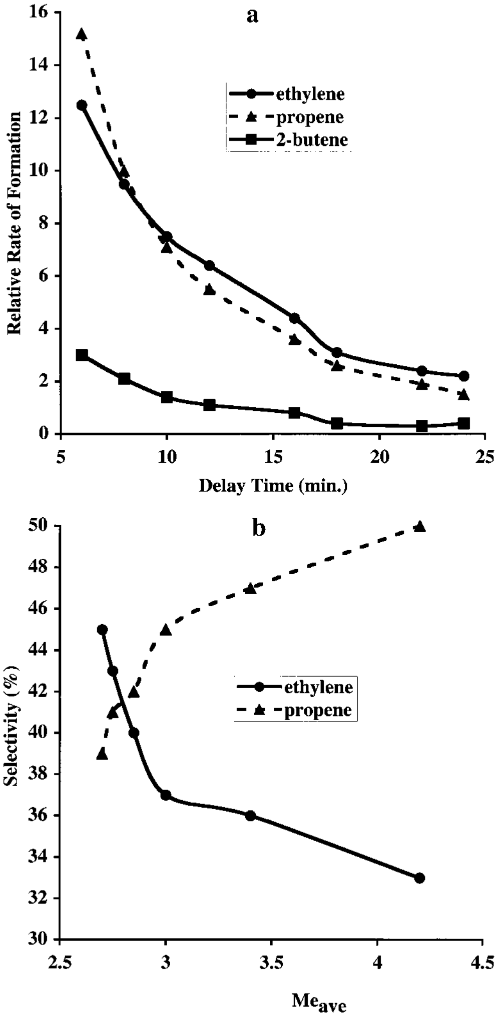

Figure 3. (a) The rates of formation of ethylene, propene, and 2-butene as a function of time from a single experiment similar to those used for Figures 1 and 2. For these measurements, multiple gas samples were analyzed from a single catalyst bed as it evolved over time after cessation of methanol flow. Ethylene and propene are major primary products of MTO chemistry. (b) Ethylene and propene selectivity as a function of the average number of methyl groups per ring, Me$_{ave}$. The data in part b are re-plotted by using an abscissa derived by empirically fitting the time evolution of Me$_{ave}$ in Figure 1 to a smooth curve generated by Excel. This mapping shows that ethylene is favored by methylbenzenes with 2 or 3 methyl groups, while propene is favored with 4 or more methyl groups.

We varied the methanol space velocity by 4 orders of magnitude (while keeping the He flow constant) and measured the steady-state olefin selectivities (all at 400 °C and 100% conversion) reported in Figure 5a. The ethylene selectivity, which was only 25% at the highest space velocities, increased dramatically as the space velocity was reduced, and we measured an extraordinary steady-state selectivity of 63% at the lowest space velocity studied. With use of the Me$_{ave}$ measurements in Figure 4, Figure 5b maps the selectivity data in Figure 5a onto an Me$_{ave}$ coordinate. Under steady-sate conditions, in a catalyst that also contains some methanol, dimethyl ether, and water in the nanocages, the changeover in selectivity for dominance of ethylene or propene occurred at Me$_{ave}$ = 2.1 in Figure 5b compared to 2.8 without methanol, dimethyl ether, and water (Figure 3b).

We also found that for a fixed space velocity of 8 h^{-1}, Me$_{ave}$ decreased with increasing temperature, and again this correlated with higher ethylene selectivity. Figure 5 shows that at 450 °C Me$_{ave}$ was 4.3 (cf. 5.6 at 400 °C) and further dropped to 1.8 at 550 °C. The ethylene selectivities were 25% at 400 °C, 34% at 450 °C, and 50% at 550 °C.

Effect of Added Water. As the first step toward studying the decomposition of methylbenzenes in HSAPO-34 cages in the presence of other molecules, we studied the effect of added

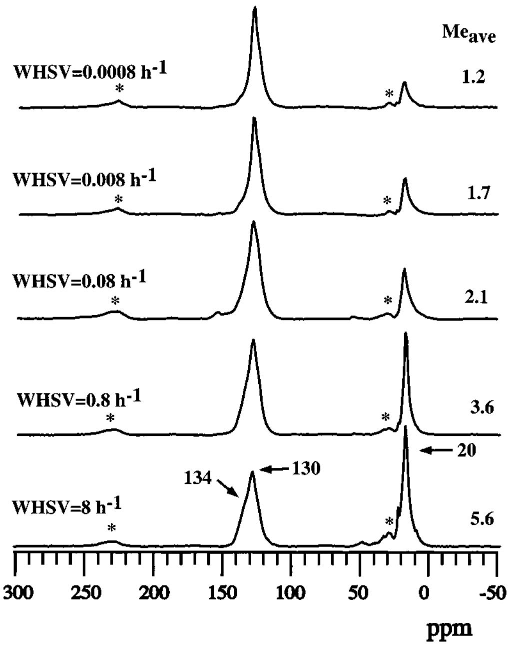

Figure 4. ^{13}C CP/MAS NMR spectra (75 MHz) from experiments probing the steady-state average number of methyl groups per ring at various methanol space velocities. In each case we converted methanol to reach steady-state selectivities, and then abruptly ceased methanol flow and thermally quenched the catalyst bed without further delay. Lower space velocities reduce the average number of methyl groups.

water at 400 °C. Water is a coproduct of MTO chemistry that must be present in at least some nanocages during methanol conversion, especially at higher space velocities. Figure 7 a,b shows that if the methanol space velocity is kept fixed but water is also introduced at a large space velocity, Me$_{ave}$ will reach a larger steady-state value, suggesting that olefin elimination is retarded by the presence of water in the cages. GC analysis of the volatile products revealed an ethylene selectivity of 35% with pure methanol delivered at 5 μL/min, but this increased to 42% when 10% (v/v) methanol in water was delivered at 50 μL/min. We also investigated the time evolution of Me$_{ave}$ following methanol cutoff *in the presence of water*. Figure 7 c shows that 60 min after cutoff Me$_{ave}$ drops to 1.9 without water, but with 10 μL/min of water following methanol cutoff (Figure 7d) Me$_{ave}$ drops to only 2.5.

Discussion

The overall kinetics of olefin synthesis on HSAPO-34 are no doubt complicated, and will vary with coadsorption of methanol, water, or other species into the nanocages containing the methylaromatics. It is convenient to consider each nanocage with a methylbenzene molecule to be a supramolecular entity, each including and delimited by the cage boundaries and possessing one acid site, but distinguished by the number of methyl groups on the benzene ring and the presence or absence of other adsorbed molecules. We will assume that equilibration of isomers is rapid compared to olefin elimination, and that we can treat, for example, a cage containing only xylene and an acid site as a single supramolecule, and not distinguish the three isomeric forms.

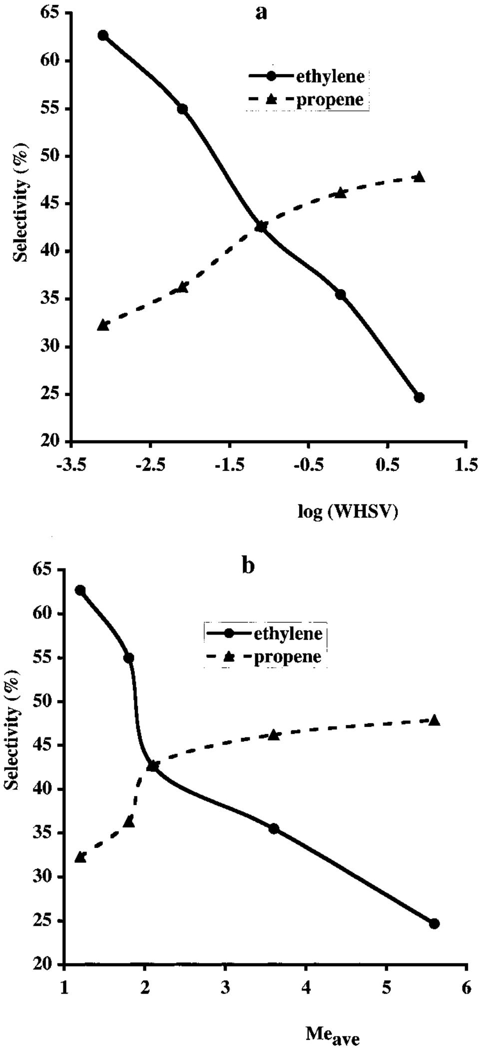

Figure 5. (a) Ethylene selectivity at 400 °C vs the logarithm of methanol weight-hourly space velocity. The catalyst bed, 300 mg, was first treated with a total of 0.1 mL of methanol at a WHSV of 8 h^{-1} at 400 °C to create methylbenzenes, and then was held at a given space velocity until selectivity reached a steady-state value. Note the very high ethylene selectivities at very low space velocities. (b) The ethylene selectivity data in part a plotted against Me$_{ave}$.

Decomposition of Methylbenzenes in HSAPO-34. The easiest case to discuss is the cutoff experiments of Figures 1−3, where there are no water or methanol molecules in the cages (at least at longer times). We can treat the decomposition of methylbenzenes to ethylene or propene and less-substituted methylbenzenes as unimolecular dissociation steps. Plots of Me$_{ave}$ versus time from experiments such as Figure 1 follow no simple integrated rate law, because of contributions from rings with different numbers of methyl groups and the time evolution of the fractions of rings, f_n, with n methyl groups. Consider the possible reactions of a trimethylbenzene molecule isolated in a nanocage. Trimethylbenzene can either lose ethylene and leave toluene with a rate constant $k(\{3\}\rightarrow\{1, e\}) = k_3^e$ or it can instead lose propene and leave benzene with a rate constant $k(\{3\}\rightarrow\{0, p\}) = k_3^p$. If all methylbenzenes function independently, and diffusion of olefin products out of the cages is rapid, then the rate of change of the average number of methyl groups per ring in an experiment like Figure 1 is described by

$$\frac{d(\mathrm{Me_{ave}})}{dt} = \sum_{n=0}^{6} n\frac{df_n}{dt} = \sum_{n=0}^{6} n[-(k_n^{e} + k_n^{p})f_n + k_n^{e}f_{n+2} + k_n^{p}f_{n+3}] \quad (2)$$

where $k_0^e = k_0^p = k_1^e = k_1^p = k_2^p = 0$, and $f_i = 0$ when $i > 6$.

Figures 1 through 3 allow us to infer the relative values of some of the rate constants. While xylene cannot eliminate

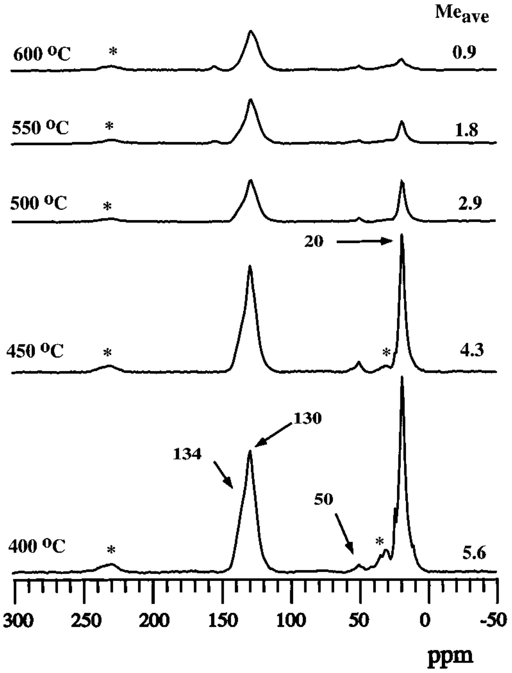

Figure 6. ^{13}C CP/MAS NMR spectra (75 MHz) probing the steady-state average number of methyl groups per ring at fixed methanol space velocity (8 h^{-1}) at various temperatures. In each case, the thermal quench occurred immediately upon cessation of methanol flow. The average number of methyl groups decreased with increasing temperature.

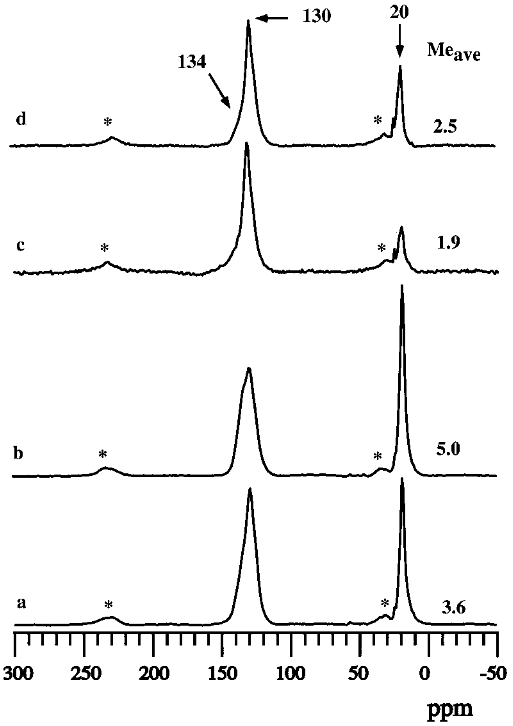

Figure 7. ^{13}C CP/MAS NMR spectra (75 MHz) from experiments probing the effect of co-feeding water on the average number of methyl groups per ring at a 400 °C reactor temperature. In every case 100 μL of pure methanol was first delivered at WHSV = 8 h^{-1} (50 μL/ min) to form methylbenzenes, and then conditions were varied: (a) control experiment, pure methanol at 5 μL/ min to reach steady-state and then thermal quench immediately upon cessation of methanol flow; (b) 10% (v/v) methanol in water at 50 μL/ min to reach steady-state and then thermal quench immediately upon cessation of flow; (c) control experiment, wait 60 min with no flow (other than He gas) after forming methylbenzenes, then thermal quench; and (d) wait 60 min while flowing 10 μL/min water with He gas after forming methylbenzenes, then thermal quench. The effect of added water is to decrease the rate of methylbenzene decomposition to olefins, hence an increase in Me$_{\mathrm{ave}}$ relative to the control experiments. Water also increases ethylene selectivity (see text).

propene, k_2^{e} is not necessarily zero. Figure 3 shows that the changeover in selectivity at 400 °C occurs with three methyl groups per ring, implying that $k_3^{\mathrm{e}} > k_3^{\mathrm{p}}$. We conclude that retention of at least one methyl group on the ring stabilizes transition states leading to olefin elimination. Also, k_6^{p} is greater than k_6^{e}, and propene is favored at higher space velocities and lower temperatures. Unfortunately, we also have the following inequalities, $k_6^{\mathrm{p}} > k_3^{\mathrm{p}}$ and $k_6^{\mathrm{e}} > k_3^{\mathrm{e}}$, and the conditions for the most rapid methanol conversion on this catalyst (large Me$_{\mathrm{ave}}$) are not those that provide the highest ethylene selectivity (small Me$_{\mathrm{ave}}$).

Temperature Effect. At higher temperatures the catalyst equilibrated to lower values of Me$_{\mathrm{ave}}$ and produced higher ethylene selectivities. Of course, this correlation does not rule out the possibility of other contributions to the temperature dependence of olefin selectivity. In a recent theoretical analysis of the elimination of ethylene and propene from another cyclic molecule, we found a higher barrier for the former relative to the latter.[4] If (as we believe) ethylbenzenes and propyl or isopropylbenzenes are precursors to olefins on HSAPO-34, elementary consideration of the stabilities of reactive intermediates would predict a higher barrier to ethylene than to propene. A higher barrier to ethylene would also contribute to improved ethylene selectivity at higher temperatures, as we observed. Thus, we suspect that both the decreased Me$_{\mathrm{ave}}$ and the greater rate of barrier crossing at higher temperatures contribute the increase in ethylene selectivity with temperature.

Effect of Water. Under realistic operating conditions of appreciable methanol space velocity, some of the cages will also contain methanol, dimethyl ether, and/or water molecules. A supramolecule consisting of a nanocage, an acid site, trimethylbenzene, and a single water molecule could still eliminate an olefin, but we would not expect, for example, $k(\{3, \mathrm{H_2O}\} \rightarrow \{1, \mathrm{H_2O}, \mathrm{e}\})$ to be identical with $k(\{3\} \rightarrow \{1, \mathrm{e}\}) = k_3^{\mathrm{e}}$, since the adsorbate would impose steric constraints, especially on the transition state, and solvate every point on the potential energy surface. (Note that a cage with trimethylbenzene and *two* water molecules would also be a distinct supramolecule with unique rate constants for decomposition to ethylene or propene.) Another possible reaction for a nanocage containing a methylbenzene and water is demethylation to form methanol, but this can be ruled out based on the endothermicity of such reactions in the gas phase. For example, the reaction of toluene and water to form benzene and methanol has a ΔH of +17.7 kcal/mol, implying a negligible equilibrium constant.[11]

The results in Figure 7 can most easily be interpreted in the context of $k(\{n, \mathrm{H_2O}\} \rightarrow \{n - 2, \mathrm{H_2O}, \mathrm{e}\}$ and $k(\{n, \mathrm{H_2O}\} \rightarrow \{n - 3, \mathrm{H_2O}, \mathrm{p}\})$ relative to the corresponding rate constants in the absence of water. Figure 7 implies that the rates of both ethylene and propene production are lower with water in the nanocages. Furthermore, the additional steric constraints provided by adsorbed water provide the most likely explanation for the increased ethylene selectivity in the water co-feed experiments.

In the more general case of a catalyst operating at appreciable methanol apace velocity we also have reactions such as $\{n, \mathrm{CH_3OH}\} \rightarrow \{n + 1, \mathrm{H_2O}\}$. The analogous reaction with dimethyl ether would produce a methanol molecule. Furthermore, me-

---

(11) NIST Chemistry WebBook (http://webbook.nist.gov/chemistry/).

thylation could occur on the side chains to more directly give precursors to ethylene or propene, but we do not consider the detailed mechanism of olefin formation in this contribution. The interplay between these various reactions, equilibration of methanol, dimethyl ether, and water, and mass transport of reactants and products through the catalyst are reflected in observables such as Me_{ave} and ethylene selectivity.

Conclusions

This investigation has found the origins of product selectivity in methanol-to-olefin chemistry on HSAPO-34. At 400 °C nanocages containing only methylbenzenes preferentially yield ethylene when the aromatic ring has two or three methyl groups, while four to six methyl groups are more likely to lead to propene as a product. This insight directly led us to significant improvements in ethylene selectivity by either reducing the methanol space velocity or increasing the temperature: we showed that either change reduces the average number of methyl groups per ring at steady-state. We partially interpreted the kinetics of this process by focusing on the unimolecular decomposition of methylbenzenes in the nanocages viewed as the reaction of one supramolecule forming another, for example $\{n\} \rightarrow \{n - 2, \mathrm{e}\}$.

Coadsorption of water produces distinct supramolecular species, for example $\{n, H_2O\}$, and these form olefins more slowly than the corresponding species without water, $\{n\}$. Co-feeding of water during methanol conversion results in an increase in the average value of n (Me_{ave}) in the catalyst when steady state is reached between methanol introduction and olefin formation. The presence of H_2O in the nanocage shifts the selectivity in favor of ethylene: the product formed through the smallest transition state.

We believe that the present study is a major step forward in the understanding of an important problem in heterogeneous catalysis. Also, the level of integration of volatile product analysis and NMR data on the solid catalyst structure (Figures 3b and 5b) represents a methodological advance. Supplementary analysis by GC has become commonplace in NMR studies of catalysis, but these data are not typically combined to the extent or advantage demonstrated here.

Acknowledgment. J.F.H. is supported by the National Science Foundation (CHE-9996109) and the U.S. Department of Energy (DOE) Office of Basic Energy Sciences (BES) (Grant No. DE-FG03-93ER14354).

JA0041167